

Available potential energy and buoyancy variance in horizontal convection

KRAIG B. WINTERS^{1,2†} AND WILLIAM R. YOUNG¹

¹Scripps Institution of Oceanography, University of California San Diego, La Jolla, CA 92093-0209, USA

²Mechanical and Aerospace Engineering, University of California San Diego, La Jolla, CA 92093-0209, USA

(Received 6 November 2008 and in revised form 24 February 2009)

We consider the mechanical energy budget for horizontal Boussinesq convection and show that there are two distinct energy pathways connecting the mechanical energy (i.e. kinetic, available potential and background potential energies) to the internal energy reservoir and the external energy source. To obtain bounds on the magnitudes of the energy transfer rates around each cycle, we first show that the volume-averaged dissipation rate of buoyancy variance $\chi \equiv \kappa \langle |\nabla b|^2 \rangle$, where b is the buoyancy, is bounded from above by $4.57h^{-1}\kappa^{2/3}\nu^{-1/3}b_{max}^{7/3}$. Here h is the depth of the container, κ the molecular diffusion, ν the kinematic viscosity and b_{max} the maximum buoyancy difference that exists on the surface. The bound on χ is used to estimate the generation rate of available potential energy E_a and the rate at which E_a is irreversibly converted to background potential energy via diapycnal fluxes, both of which are shown to vanish at least as fast as $\kappa^{1/3}$ in the limit $\kappa \rightarrow 0$ at fixed Prandtl number $Pr = \nu/\kappa$. As a thought experiment, consider a hypothetical ocean insulated at all boundaries except at the upper surface, where the buoyancy is prescribed. The bounds on the energy transfer rates in the mechanical energy budget imply that buoyancy forcing alone is insufficient by at least three orders of magnitude to maintain observed oceanic dissipation rates and that additional energy sources such as winds, tides and perhaps bioturbation are necessary to sustain observed levels of turbulent dissipation in the world's oceans.

1. Introduction

In a horizontally convective flow, heating and cooling are applied at a single level. This is a classical model of the buoyancy-forced ocean circulation (Sandström 1908; Jeffreys 1925; Rossby 1965; Stern 1975). Spurred by Munk & Wunsch's discussion of the energy sources of ocean turbulence (Munk & Wunsch 1998), there has been substantial experimental and theoretical work on horizontal convection in the last decade. This progress is reviewed by Hughes & Griffiths (2008), who conclude their discussion of thermodynamics by remarking that the energetics of horizontal convection is still an open issue.

A general result concerning the energetics of horizontal convection is Paparella & Young's demonstration (Young 2002) that in horizontal convection the rate of transformation of potential energy into kinetic energy is directly proportional to the molecular thermal diffusivity κ (see (2.10)). This result is a precise version of Jeffreys'

† Email address for correspondence: kraig@coast.ucsd.edu

argument (Jeffreys 1925) that molecular diffusion enables internal penetration of surface temperature variations, so that the heating and cooling of circulating fluid elements can occur at different pressures. Thus Sandström's Carnot-cycle arguments (Sandström 1908), which assume that heating is strictly at the surface, are not valid. As an antidote, Nycander *et al.* (2007) provided a modern thermodynamic view of the overturning circulation of the ocean. But the point remains that because κ is small, the interior penetration of heating is confined to a thin surface boundary layer, and the resulting energy source is feeble. In this narrow sense Sandström's intuition is correct (Sandström 1908). In fact, using one definition of turbulence, (2.10) implies that steady horizontal convective flows are not turbulent in the bulk. There is, however, the possibility of turbulence in a small part of the domain e.g. in localized plumes.

Following Bjerknes (1916), Sandström's thermodynamic ruminations (Sandström 1908) unfortunately came to be known as Sandström's theorem, which claimed that differential heating applied at a single level cannot drive a circulation. This conclusion, influentially endorsed in Defant's textbook (Defant 1961), is false on several grounds. Not the least of these is that experiments clearly show a circulation (e.g. Rossby 1965; Mullarney, Griffiths & Hughes 2004; Wang & Huang 2005; Coman, Griffiths & Hughes 2006). Thus it is important to realize that (2.10) constrains neither the strength of the overturning circulation nor the heat transport. The quest here is for additional integral constraints that probe these important quantities, and thus we develop further thermodynamic arguments, based on dissipation of buoyancy variance and generation of available potential energy.

2. Formulation and the mechanical energy balance

We consider a three-dimensional rotating fluid in a rectangular box of volume V with horizontal cross-sectional area A and uniform depth h ; the vertical coordinate is $0 \leq z \leq h$. The density is expressed as $\rho = \rho_0(1 - g^{-1}b)$, where b is the 'buoyancy'. The Boussinesq equations of motion are then

$$\frac{D\mathbf{u}}{Dt} + 2\boldsymbol{\Omega} \times \mathbf{u} + \nabla p = b\hat{\mathbf{z}} + \nu\nabla^2\mathbf{u}, \quad (2.1)$$

$$\frac{Db}{Dt} = \kappa\nabla^2 b, \quad (2.2)$$

$$\nabla \cdot \mathbf{u} = 0. \quad (2.3)$$

The pressure is $\rho_0 p$, and $\boldsymbol{\Omega}$ is the rotation vector. The boundary conditions on $\mathbf{u} = (u, v, w)$ are $\mathbf{u} \cdot \hat{\mathbf{n}} = 0$, where $\hat{\mathbf{n}}$ is the outward normal to the surface of V , and some combination of no slip and no stress. The buoyancy is specified at the top surface

$$b(x, y, h) = b_s(x, y), \quad \text{with} \quad 0 \leq b_s(x, y) \leq b_{max}. \quad (2.4)$$

On the other five faces of V , there is no flux of buoyancy i.e. $\nabla b \cdot \hat{\mathbf{n}} = 0$. Throughout, we use the phrase 'horizontal convection' to refer to the idealized problem defined by (2.1)–(2.3) along with the boundary conditions described above.

We denote a space–time average over the horizontal coordinates x and y , and time t , by an overbar; e.g. $\bar{b}(z)$ is the horizontally averaged buoyancy. Two important constraints are obtained by horizontally averaging (2.2):

$$\overline{wb} - \kappa\bar{b}_z = 0 \quad \text{and} \quad \kappa\bar{b}_z(h) = 0. \quad (2.5)$$

In (2.5), the subscript z indicates partial differentiation with respect to z . The first result in (2.5) is the zero-flux constraint, saying that there is no net vertical flux of buoyancy

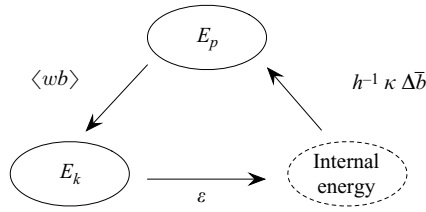


FIGURE 1. Energy cycle between mechanical and internal energies for steady, or statistically steady, horizontal convection.

at every level z . Evaluating the zero-flux constraint at $z = h$ gives the second result in (2.5): in statistical steady state there is no net input of buoyancy through the surface.

The kinetic and potential energies per unit mass may be defined via the integrals

$$E_k(t) \equiv \frac{1}{2} \int |\mathbf{u}|^2 dV \quad \text{and} \quad E_p(t) \equiv \int (h - z)b dV. \tag{2.6}$$

Evolution equations for E_k and E_p are derived from the equations of motion (2.1)–(2.3) and are given for general boundary conditions in Winters *et al.* (1995). For the boundary conditions of horizontal convection, the energy equations in Winters *et al.* (1995) reduce to

$$\frac{dE_p}{dt} = - \int w b dV + \kappa \int b \hat{\mathbf{z}} \cdot \hat{\mathbf{n}} dA, \tag{2.7}$$

$$\frac{dE_k}{dt} = \int w b dV - \nu \int (|\nabla \mathbf{u}|^2 + |\nabla v|^2 + |\nabla w|^2) dV. \tag{2.8}$$

Taking the time and volume averages of the equations above produces two expressions for the vertical buoyancy flux:

$$\langle wb \rangle = \varepsilon \quad \text{and} \quad \langle wb \rangle = \frac{\kappa}{h} \Delta \bar{b}, \tag{2.9}$$

where $\Delta \bar{b} \equiv \bar{b}(h) - \bar{b}(0)$ and where $\langle \rangle$ denotes the average over V . In (2.9), the kinetic energy dissipation is $\varepsilon \equiv \nu \langle |\nabla \mathbf{u}|^2 + |\nabla v|^2 + |\nabla w|^2 \rangle$. The surface boundary condition (2.4) has not been used to obtain (2.9): thus these balances apply more generally to horizontal convection with fixed-flux or relaxation conditions at $z = h$.

The balances in (2.9) quantify the rate of production of E_p , the conversion from E_p to E_k and the rate of kinetic energy dissipation. Independent of the exact form of $b_s(x, y)$, each of these energy transfer rates has a magnitude of $\kappa \Delta \bar{b} / h$. Because the largest and smallest values of b are on the surface $z = h$, (2.4) yields a bound on the average dissipation rate:

$$\varepsilon \leq \frac{\kappa}{h} b_{max}. \tag{2.10}$$

With fixed buoyancy at the surface and therefore known b_{max} , the anti-turbulence theorem of Paparella & Young (2002) follows: in the limit $\nu \rightarrow 0$ with fixed $Pr \equiv \nu / \kappa$, the volume-averaged dissipation rate ε vanishes.

Neither the bound (2.10) nor the mechanical energy budget (2.9) say anything about the rate at which energy is externally supplied via surface buoyancy flux or the rate at which energy is irreversibly converted to background potential energy via diapycnal mixing. In fact, one can regard the energy conversion rates of (2.9) as a closed energy cycle (see figure 1) in which energy is exchanged between internal and mechanical forms in the Boussinesq limit (Winters *et al.* 1995; Wang & Huang 2005).

Moreover, the energy transfers in this cycle are weak. For example, one can use the bound (2.10) to estimate the maximum ε that might be sustained by non-uniform surface buoyancy flux alone under oceanic conditions. If $b_{max} = 5 \times 10^{-2} \text{ m s}^{-2}$, corresponding to a temperature difference of 25 K and an expansion coefficient of $2 \times 10^{-4} \text{ K}^{-1}$, $h = 5000 \text{ m}$ and $\kappa = 10^{-7} \text{ m}^2 \text{ s}^{-1}$, then

$$\varepsilon \leq 1 \times 10^{-12} \text{ W kg}^{-1}. \tag{2.11}$$

The observed level of small-scale turbulence in the ocean interior is $\varepsilon \sim 10^{-9} \text{ W kg}^{-1}$, which is greater than (2.11) by three orders of magnitude. Notice that the estimate (2.11) can be made using an observed b_{max} and therefore is not hostage to the fixed-buoyancy boundary condition in (2.4).

3. Buoyancy variance and its dissipation

If (2.2) is multiplied by b and integrated over the volume one has

$$\frac{d}{dt} \int \frac{b^2}{2} dV = \int b_s \kappa b_z dA_{z=h} - \kappa \int |\nabla b|^2 dV. \tag{3.1}$$

Time and volume averaging the buoyancy variance equation above, one has

$$\chi = \frac{\kappa}{h} \overline{b_s b_z(h)}, \quad \text{where} \quad \chi \equiv \kappa \langle |\nabla b|^2 \rangle. \tag{3.2}$$

Notice that buoyancy variance is forced by the correlation between the imposed surface buoyancy $b_s(x, y)$ and the unknown surface buoyancy flux $\kappa b_z(x, y, h, t)$. Because $\chi > 0$, (3.2) shows that the correlation is positive.

The measure of how strongly buoyancy variance is cascaded into small dissipation scales by the flow is χ , and it also is the most basic measure of the advective intensification of buoyancy gradients and vertical mixing (Osborn & Cox 1972). More detailed information than the single number χ is provided by the function $\phi_d(b)$; following Winters & D’Asaro (1996) $\phi_d(b)$ is the normalized and averaged flux of buoyancy across the buoyancy surface S_b ,

$$\phi_d(b) \equiv \frac{1}{AT} \int_0^T \int \kappa |\nabla b| dS_b dt, \tag{3.3}$$

where A is the horizontal cross-sectional area of the box. Noting that $dV = dS_b db / |\nabla b|$, one can show that

$$\chi = \frac{1}{h} \int_0^{b_{max}} \phi_d(b) db. \tag{3.4}$$

In this section we obtain a rigorous bound on χ , implying that

$$\lim_{\kappa \rightarrow 0} \chi = 0. \tag{3.5}$$

Because $\phi_d(b) \geq 0$ for all b , the identity (3.4) implies that the average buoyancy flux through every buoyancy surface vanishes as $\kappa \rightarrow 0$.

3.1. A bound on χ as $\kappa \rightarrow 0$ at fixed Pr : heuristic considerations

To motivate our approach, note that the limit in (3.5) does not follow immediately from (3.2) because we cannot eliminate the possibility that b develops very small scales near $z = h$, so that a boundary layer with a thickness proportional to κ is created; i.e. b_z in (3.2) might be as large as $O(\kappa^{-1})$. This very thin layer could, in

principle, result in a non-zero injection of buoyancy variance and non-zero χ , even as $\kappa \rightarrow 0$. This is a very real possibility in Rayleigh–Bénard convection (Siggia 1994).

At a heuristic level one can argue that the smallest conceivable boundary layer thickness δ is determined by concentrating all of the energy dissipation bounded by (2.10) in the layer and that there is a balance $\delta \sim \nu/U$, where U is the characteristic magnitude of the velocity difference across the layer. The energy dissipation in this hypothetical boundary layer scales as $\varepsilon_\delta \equiv \nu(U/\delta)^2$, and since the layer occupies a fraction δ/h of the total volume, the volume-averaged dissipation is

$$\varepsilon \sim \frac{\delta}{h} \varepsilon_\delta \sim \frac{U^3}{h}. \tag{3.6}$$

Equating the estimate above to ε in (2.10), one obtains

$$U \sim (\kappa b_{max})^{1/3} \quad \text{and} \quad \delta \sim \frac{\nu}{(\kappa b_{max})^{1/3}} = \frac{Pr \kappa^{2/3}}{b_{max}^{1/3}}, \tag{3.7}$$

where $Pr \equiv \nu/\kappa$ is the Prandtl number. Taking the limit $\kappa \rightarrow 0$, with Pr fixed, indicates that the thinnest possible boundary layer scales as

$$\delta \propto \kappa^{2/3} \gg \kappa. \tag{3.8}$$

For comparison, Rossby’s (1965) boundary layer has a thickness scaling as $\kappa^{2/5}$, which is much larger than δ above. The heuristic argument leading to (3.8) indicates that, because of the feeble supply of kinetic energy, it is not possible to create a boundary layer with thickness as small as κ and therefore not possible to supply a finite non-zero χ in the limit $\kappa \rightarrow 0$. In fact, using the estimates $b_s \leq b_{max}$ and $b_z \lesssim b_{max}/\delta$ in the right-hand side of (3.2) we have

$$\chi \lesssim \frac{\kappa b_{max}^2}{\delta} \sim \frac{\kappa^{1/3} b_{max}^{7/3}}{h Pr}. \tag{3.9}$$

With this motivation, we turn to a rigorous version of these estimates.

3.2. A bound on χ as $\kappa \rightarrow 0$ at fixed Pr : the comparison function method

To obtain rigorous versions of (3.8) and (3.9) we follow Balmforth & Young (2003) and introduce a ‘comparison function’ $c(\mathbf{x})$ that satisfies the same boundary conditions as $b(\mathbf{x}, t)$ and has other desirable properties outlined below. In analogy with the right-hand side of (3.2), we define

$$\chi_c \equiv \frac{\kappa}{h} \overline{b_s c_z(h)}. \tag{3.10}$$

Multiplying (2.2) by $c(\mathbf{x})$, space–time averaging and using Green’s second theorem with $c = b_s$ at the surface, one obtains

$$\chi = \chi_c - \langle \mathbf{b} \mathbf{u} \cdot \nabla c \rangle - \kappa \langle \mathbf{b} \nabla^2 c \rangle. \tag{3.11}$$

The salient property of (3.11) is that the right-hand side does not involve derivatives of b . Thus, invoking the extremum principle

$$0 \leq b \leq b_{max}, \tag{3.12}$$

we obtain the upper bound:

$$\chi \leq \chi_c + b_{max} [\langle |u| |c_x| \rangle + \langle |v| |c_y| \rangle + \langle |w| |c_z| \rangle + \kappa \langle |\nabla^2 c| \rangle]. \tag{3.13}$$

With (3.13) we can bound χ from above, knowing nothing about ∇b .

As a comparison function we now introduce

$$c(\mathbf{x}) = \frac{\cosh(\mu z)}{\cosh \mu h} b_s(x, y); \tag{3.14}$$

$c(\mathbf{x})$ above satisfies the same boundary conditions as $b(\mathbf{x}, t)$ at $z=0$ and $z=h$. To secure the lateral boundary conditions on $c(\mathbf{x})$, we make the non-essential assumption that $b_s(x, y)$ satisfies no-flux boundary conditions on the walls of the container. The parameter μ in (3.14) is at our disposal and is used below to obtain the minimum upper bound on χ attainable using this approach. In fact, we now limit attention to large values of μ so that $c(\mathbf{x})$ is non-zero only in a boundary layer of thickness μ^{-1} clinging to $z=h$, and in this sheath

$$c(x, y, z) \approx e^{\mu(z-h)} b_s(x, y). \tag{3.15}$$

It is now straightforward to obtain an upper bound on the right-hand side of (3.13). The main point is that z -derivatives of c are of order μ but only in a boundary layer of thickness μ^{-1} ; i.e. the interior of the box does not contribute. All the horizontal derivatives of c are asymptotically negligible.

The easiest term is χ_c defined in (3.10):

$$\chi_c \approx \kappa \mu h^{-1} \overline{b_s^2} \leq \kappa \mu h^{-1} b_{max}^2. \tag{3.16}$$

The term $\kappa \langle |\nabla^2 c| \rangle$ on the right-hand side of (3.13) is also easy: $\nabla^2 c \approx \mu^2 c$, and one has

$$\kappa \langle |\nabla^2 c| \rangle \approx \kappa \mu h^{-1} \langle |b_s| \rangle \leq \kappa \mu h^{-1} b_{max}. \tag{3.17}$$

To obtain useful estimates of the advective term $\langle |w| |c_z| \rangle$ in (3.13), one must bound $|w|$. Because w vanishes at $z=0$ and h , the largest possible value of $|w|$ in the interior of the domain must somehow be bounded by the root mean square of w_z :

$$\omega(x, y, t) \equiv \sqrt{\frac{1}{h} \int_0^h w_z^2 dz}. \tag{3.18}$$

For example, if ω is zero, then w must vanish everywhere, and if ω is small, then w can't be very large, even in the middle of the domain. Howard's Lemma 1 (Howard 1972), that

$$w(\mathbf{x}, t) \leq \sqrt{z(h-z)} \omega(x, y, t), \tag{3.19}$$

provides a rigorous basis for these intuitive expectations. Howard's inequality (3.19) (Howard 1972), along with

$$|c_z(\mathbf{x})| \leq \mu b_{max} e^{\mu(z-h)}, \tag{3.20}$$

implies that

$$\langle |w| |c_z| \rangle \leq \mu \langle \omega \rangle \langle \sqrt{z(h-z)} e^{\mu(z-h)} \rangle b_{max} \tag{3.21}$$

$$\leq \mu \sqrt{\langle \omega^2 \rangle} \langle \sqrt{z(h-z)} e^{\mu(z-h)} \rangle b_{max}, \tag{3.22}$$

$$\leq \frac{3}{2} \sqrt{\frac{\pi \langle w_z^2 \rangle}{\mu h}} b_{max}. \tag{3.23}$$

The Cauchy–Schwarz inequality $\langle \omega \rangle \leq \sqrt{\langle \omega^2 \rangle}$ has been used to pass from (3.21) to (3.22). Between (3.22) and (3.23) we have used $\langle \omega^2 \rangle = \langle w_z^2 \rangle$ and

$$\langle \sqrt{z(h-z)} e^{\mu(z-h)} \rangle \approx \frac{3}{2} \sqrt{\frac{\pi}{h\mu^3}}. \tag{3.24}$$

The horizontal advective terms on the right-hand side of (3.13) can be estimated using the x and y analogues of Howard’s (1963) lemma. These contributions however are negligible relative to $\langle |w||c_z| \rangle$ as $\mu h \rightarrow \infty$.

Collecting the estimates above, the bound in (3.13) is

$$\chi \leq b_{max}^2 \left[2 \frac{\kappa m}{h^2} + \frac{3}{2} \sqrt{\frac{\pi \langle w_z^2 \rangle}{m}} \right], \tag{3.25}$$

where $m \equiv \mu h$. Next, since $\langle w_z^2 \rangle \leq \varepsilon / \nu$,

$$\chi \leq b_{max}^2 \left[2 \frac{\kappa m}{h^2} + \frac{3}{2} \sqrt{\frac{\pi \varepsilon}{\nu m}} \right]. \tag{3.26}$$

Finally, we minimize the right-hand side of (3.25) over m . The optimal value

$$m_* = \left(\frac{3\sqrt{\pi}}{8} \sqrt{\frac{\varepsilon}{\nu}} \frac{h^2}{\kappa} \right)^{2/3} \tag{3.27}$$

results in the bound

$$\chi \leq 4.57 \left(\frac{\kappa}{\nu} \frac{\varepsilon}{h^2} \right)^{1/3} b_{max}^2, \tag{3.28}$$

where the numerical constant is $3^{5/3} \pi^{1/3} / 2 \approx 4.57$.

Inequality (3.28) shows that χ is limited from above by the inverse time scale $(\varepsilon/h^2)^{1/3}$. Consequently if $\varepsilon \rightarrow 0$ with κ , then so does χ . In particular, the bound $\varepsilon \leq b_{max} \kappa / h$ implies that for horizontal convection

$$\chi \leq 4.57 \frac{\kappa^{1/3} b_{max}^{7/3}}{Pr^{1/3} h}. \tag{3.29}$$

The bound (3.29) is almost in agreement with (3.9): both approaches yield estimates with a boundary layer thickness $\delta \propto m_*^{-1} \propto \kappa^{2/3}$. This forces the conclusion that χ vanishes at least as fast as $\kappa^{1/3}$ as $\kappa \rightarrow 0$ for fixed Pr . The difference between (3.29) and (3.9) is a factor $Pr^{2/3}$. (If one initially took the boundary thickness as $\delta = \kappa / U$ in the heuristic argument, then (3.29) and (3.9) differ only by the numerical constant 4.57.)

To conclude this section we note that (3.28) does not take advantage of any potential cancellation, such as that in $\kappa \bar{b}_z(h) = 0$. Instead, we have used inequalities that very crudely estimate the maximum possible magnitude of the various terms in the comparison function bound on χ . Thus, unlike the bound on ε in (2.10), the upper bound on χ is likely generously large.

4. The available potential energy cycle of horizontal convection

We turn now to the available potential energy cycle specialized to horizontal convection (see also Hughes, Hogg & Griffiths 2008). The first step is to decompose the total potential energy, E_p in (2.6), into available and background components and consider the evolution equations for the components separately. This is accomplished

by defining the background potential energy as the minimum potential energy achievable via adiabatic rearrangement of infinitesimal fluid parcels. To this end, we define $z_*(b, t)$ to be the reference height in the minimum potential energy state of fluid with buoyancy $b(\mathbf{x}, t)$. As discussed in Winters *et al.* (1995),

$$z_*(b, t) = \frac{1}{A} \int H[b(\mathbf{x}, t) - b(\mathbf{x}', t)] dV', \quad (4.1)$$

where H is the Heaviside step function; $0 \leq z_* \leq h$ is a unique function of b .

The background potential energy E_b , defined by analogy with E_p in (2.6), is then

$$E_b \equiv \int (h - z_*) b dV, \quad (4.2)$$

and we define the available potential energy as $E_a \equiv E_p - E_b$.

For horizontal convection, the evolution equation for background potential energy from Winters *et al.* (1995) is

$$\frac{dE_b}{dt} = \kappa \int \frac{dz_*}{db} |\nabla b|^2 dV + \kappa \int (h - z_*) b_z dA_{z=h}. \quad (4.3)$$

The equation for E_a is obtained by subtracting (4.3) from (2.7):

$$\frac{dE_a}{dt} = - \int w b dV + \kappa \int b \hat{z} \cdot \hat{n} dA - \kappa \int \frac{dz_*}{db} |\nabla b|^2 dV - \kappa \int (h - z_*) b_z dA_{z=h}. \quad (4.4)$$

The first term on the right-hand side of (4.4) is the rate at which kinetic energy is converted to available potential energy through advective buoyancy flux. The second and third terms, taken together and discussed further below, quantify the rate at which available potential energy is converted to background potential energy via diapycnal buoyancy flux, i.e. irreversible mixing. The last terms in (4.3) and (4.4) give the rate at which surface buoyancy fluxes decrease/increase the background/available potential energy of the system respectively.

The balances in (4.3) and (4.4) simplify after space-time averaging. Using (2.5) and (2.9), the steady state budget for available and background potential energy reduce to

$$\Phi_d = \frac{\kappa}{h} \overline{z_*(b_s) b_z(h)}, \quad \text{where} \quad \Phi_d \equiv \kappa \left\langle \frac{dz_*}{db} |\nabla b|^2 \right\rangle \geq 0. \quad (4.5)$$

The result above is analogous to (3.2), and again we face the problem that the surface source on the right-hand side of (4.5) depends on the unknown surface flux $\kappa b_z(x, y, h, t)$.

The balance (4.5), in combination with (2.9), suggests that we view the energy budgets of horizontal convection in terms of two closed cycles that link the mechanical energy to both internal and external energy reservoirs, as shown in figure 2. The upper cycle describes the energy transfers between external and mechanical energies and, more specifically, between external, available and background potential energies.

At this point, (4.5) and (2.9) provide exact expressions quantifying the energy transfers through both cycles in figure 2, but we have a useful bound (2.10) only on the transfer through the lower cycle. To constrain the strength of upper cycle, we estimate the right-hand side of (4.5) using $z_* \leq h$ and $b_z \lesssim b_{max}/\delta$, where δ is the upper boundary layer thickness. Thus

$$\Phi_d \lesssim \frac{\kappa b_{max}}{\delta} \sim \frac{\kappa^{1/3} b_{max}^{4/3}}{Pr}, \quad (4.6)$$

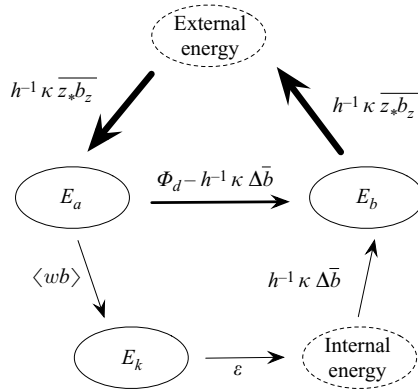


FIGURE 2. Energy cycle between mechanical, external and internal energies for steady, or statistically steady, horizontal convection. The bound on the lower cycle (cf. (2.10)) is rigorous, while that on the upper cycle (cf. (4.6)) is approximate.

where in the second inequality we've used the estimate of δ in (3.7). Because of the heuristic estimate of δ (4.6) is not a rigorous upper bound on Φ_d . But in view of the agreement between (3.29) and (3.9), the estimate of δ in (4.6) is very plausible.

5. Discussion and conclusions

We have shown that the energy budget of horizontal convection consists of two distinct energy pathways that branch from the available potential energy reservoir as shown in figure 2. Consideration of the total mechanical energy budget allows rigorous bounding of only the lower cycle associated with kinetic and internal energies. In the case of the upper cycle, which exposes the exchanges with the external source, the bound (4.6) is not rigorous, but it is very plausible. Thus the rate of energy transfer around both cycles vanishes in the limit $(\kappa, \nu) \rightarrow 0$ at fixed Pr . Moreover the dissipation of buoyancy variance χ is rigorously bounded in (3.29) so that $\chi \rightarrow 0$ with κ . These bounds highlight the role of the surface boundary layer as a bottleneck in horizontal convection: because the boundary layer thickness is significantly thicker than $O(\kappa)$ it is not possible to inject non-zero available potential energy and buoyancy variance into a steady horizontally convective flow as $\kappa \rightarrow 0$.

As in (2.11), the bound on ε is small compared to observed oceanic values. These results imply then, in the absence of additional energy sources, surface buoyancy forcing alone is incapable of driving a circulation with dissipation rates comparable to those observed, consistent with the interpretation of Hughes *et al.* (2008) based on their analysis of available potential energy. We argue that this conclusion is inescapable from (2.10) and consistent with the widely accepted hypothesis that ε in the bulk of the ocean is due primarily to breaking internal gravity waves, with marine bioturbation (Dewar *et al.* 2006) a second, speculative possibility. Winds and tides are prime and direct generators of internal waves (Munk & Wunsch 1998), and thus it is natural that a combination of surface stresses and body forces must be added to the idealized horizontal convection model to force gravity waves and develop a circulation with a realistic value of ε .

This work was supported by the National Science Foundation (grant number OCE07-26320) and the Office of Naval Research (grant number N00014-05-1-0573).

We thank Neil Balmforth, Ross Griffiths, Andy Hogg, Graham Hughes, Michael McIntyre, Francesco Paparella and Rémi Tailleux for comments and discussion.

REFERENCES

- BALMFORTH, N. J. & YOUNG, W. R. 2003. Diffusion-limited scalar cascades. *J. Fluid Mech.* **482**, 91–100.
- BJERKNES, V. 1916. Über thermodynamische Maschinen, die unter Mitwirkung der Schwerkraft arbeiten. *Abh. Akad. Wissensch. Leipzig* **35** (1), 1–33.
- COMAN, M. A., GRIFFITHS, R. W. & HUGHES, G. O. 2006 Sandström's experiments revisited. *J. Mar. Res.* **64**, 783–796.
- DEFANT, A. 1961 *Physical Oceanography*, vol. 1. MacMillan.
- DEWAR, W. K., BINGHAM, R. J., IVERSON, R. L., NOWACEK, D. P., ST. LAURENT, L. C. & WIEBE, P. H. 2006 Does the marine biosphere mix the ocean? *J. Mar. Res.* **64**, 541–561.
- HOWARD, L. N. 1972 Bounds on flow quantities. *Annu. Rev. Fluid Mech.* **17**, 473–494.
- HUGHES, G. O. & GRIFFITHS, R. W. 2008 Horizontal convection *Annu. Rev. Fluid Mech.* **40**, 185–208.
- HUGHES, G. O., HOGG, A. M. & GRIFFITHS, R. W. 2008 Available potential energy and irreversible mixing in the meridional overturning circulation *J. Phys. Oceanogr.* Submitted.
- JEFFREYS, H. 1925 On fluid motions produced by differences of temperature and humidity. *Quart. J. R. Meteorol. Soc.* **51**, 347–356.
- MULLARNEY, J. C., GRIFFITHS, R. W. & HUGHES, G. O. 2004. Convection driven by differential heating at a horizontal boundary. *J. Fluid Mech* **516**, 181209.
- MUNK, W. H. & WUNSCH, C. 1998 Abyssal recipes. Part 2. Energetics of tidal and wind mixing. *Deep-Sea Res.* **45**, 1977–2010.
- NYCANDER, J., NILSSON, J., DÖÖS, K. & BROSTRÖM 2007 Thermodynamic analysis of ocean circulation. *J. Phys. Oceanogr.* **37**, 2038–2052.
- OSBORN, T. R. & COX, C. S. 1972 Oceanic fine structure. *Geophys. Fluid Dyn.* **3**, 321–345.
- PAPARELLA, F. & YOUNG, W. R. 2002 Horizontal convection is non-turbulent. *J. Fluid Mech.* **466**, 205–214.
- ROSSBY, T. 1965 On thermal convection driven by non-uniform heating from below: an experimental study. *Deep-Sea Res.* **12**, 9–16.
- SANDSTRÖM, J. W. 1908 Dynamische Versuche mit Meerwasser. *Ann. Hydrodyn. Mar. Meteorol.* **36**, 6–23.
- SIGGIA, E. D. 1994 High Rayleigh number convection. *Annu. Rev. Fluid Mech.* **26**, 137–168.
- STERN, M. E. 1975 *Ocean Circulation Physics*. International Geophysics Series, vol. 19. Academic.
- WANG, W. & HUANG, R. X. 2005. An experimental study on thermal convection driven by horizontal differential heating. *J. Fluid Mech* **540**, 4973.
- WINTERS, K. B. & D'ASARO, E. A. 1996. Diascalar flux and the rate of fluid mixing. *J. Fluid Mech.* **317**, 179–193.
- WINTERS, K. B., LOMBARD, P. N., RILEY, J. J. & D'ASARO, E. A. 1995. Available potential energy and mixing in density stratified fluids. *J. Fluid Mech.* **289**, 115–128.